

# Quantum assisted quantum compiling

Sumeet Khatri,<sup>1,2,\*</sup> Ryan LaRose,<sup>1,3,\*</sup> Alexander Poremba,<sup>1,\*</sup>  
Lukasz Cincio,<sup>1</sup> Andrew T. Sornborger,<sup>4</sup> and Patrick J. Coles<sup>1</sup>

<sup>1</sup>*Theoretical Division, Los Alamos National Laboratory, Los Alamos, NM 87545, USA.*

<sup>2</sup>*Hearne Institute for Theoretical Physics, Department of Physics and Astronomy,  
Louisiana State University, Baton Rouge, Louisiana 70803, USA.*

<sup>3</sup>*Department of Computational Mathematics, Science,  
and Engineering & Department of Physics and Astronomy,  
Michigan State University, East Lansing, MI 48823, USA.*

<sup>4</sup>*Information Sciences, Los Alamos National Laboratory, Los Alamos, NM 87545, USA.*

Compiling quantum algorithms for near-term quantum computers (accounting for connectivity and native gate alphabets) is a major challenge that has received significant attention both by industry and academia. Avoiding the exponential overhead of classical simulation of quantum dynamics will allow compilation of larger algorithms, and a strategy for this is to evaluate an algorithm's cost on a quantum computer. Here we propose to use the Hilbert-Schmidt inner product between a target unitary  $U$  and a trainable unitary  $V$  as the cost function to be evaluated on the quantum computer. We introduce two circuits for evaluating this cost. One circuit avoids using controlled unitaries (and hence is shorter depth) and gives  $|\text{Tr}(V^\dagger U)|$ . We use this circuit for gradient-free compiling. Our other circuit gives  $\text{Tr}(V^\dagger U)$  and is a generalization of the power-of-one-qubit circuit that we call the power-of-two-qubits. We use this circuit for gradient-based compiling. We illustrate both our gradient-free and gradient-based methods by compiling various one-qubit gates to the native gate alphabets on IBM's and Rigetti's quantum computers, and we also compile multiqubit gates on a simulator.

## I. INTRODUCTION

Factoring [1], approximate optimization [2], and simulation of quantum systems [3] are some of the applications for which quantum computers have been predicted to provide speedup over classical computers. Consequently, the prospect of large-scale quantum computers has generated interest from various industries, such as the financial and pharmaceutical industries. Currently available quantum computers are not large scale but rather have been called noisy intermediate-scale quantum (NISQ) computers [4]. A proof-of-principle demonstration of quantum supremacy with a NISQ device may be coming soon [5, 6]. Nevertheless, demonstrating the practical utility of NISQ computers appears to be more difficult task.

While improvements to NISQ hardware are continuously being made by experimentalists, quantum computing theorists can contribute to NISQ utility by developing software. This software would aim to adapt textbook quantum algorithms (e.g., for factoring or quantum simulation) to NISQ constraints. NISQ constraints include: (1) limited numbers of qubits, (2) limited connectivity between qubits, (3) restricted (hardware-specific) gate alphabets, and (4) limited circuit depth due to noise. Algorithms adapted to these constraints will likely look dramatically different from their textbook counterparts.

These constraints have generated the field of quantum compiling. In classical computing, a compiler is a program that converts instructions into a machine-code or

lower-level form so that they can be read and executed by a computer. Similarly, a quantum compiler would take a high-level algorithm and convert it into one that could be executed on a NISQ device. Already, a large body of literature exists on classical approaches for quantum compiling, e.g., using temporal planning [7], machine learning [8], and other techniques [9–15].

A recent exciting idea is to use quantum computers, themselves, to assist in the quantum compiling process [16–19]. Various names have been used for this idea - we call it quantum assisted quantum compiling (QAQC). The main benefit of QAQC is that classical simulation of quantum dynamics is exponentially slower than quantum simulation. Hence, evaluating the cost of a quantum gate sequence on a quantum computer leads to an exponential speedup (in the number of qubits involved in the gate sequence). Consequently, one should be able to compile larger-scale gate sequences using QAQC, whereas classical approaches to quantum compiling will be limited to smaller gate sequences [37].

The circuit used to evaluate the cost in QAQC can itself be viewed as a quantum algorithm. This cost-evaluation circuit should ideally be as short depth as possible, since noise in NISQ hardware will lead to inaccurate cost values for deep circuits. In this work, our main contribution is to present two novel short-depth circuits for cost evaluation. We propose using one of these circuits for gradient-free QAQC (where the circuit evaluates the cost only) and the other for gradient-based QAQC (where the circuit evaluates the cost and the gradient).

Both of our circuits consider the cost to be the Hilbert-Schmidt inner product between a target unitary  $U$  and

---

\*The first three authors contributed equally to this work.

a trainable unitary  $V$ ,

$$\langle V, U \rangle = \text{Tr}(V^\dagger U). \quad (1)$$

Our first circuit, which we call the Hilbert-Schmidt Test, computes the magnitude of this inner product,  $|\langle V, U \rangle|$ . It achieves short depth by avoiding implementing controlled versions of  $U$  and  $V$ , and by implementing  $U$  and  $V$  in parallel.

Our second circuit computes the real and imaginary parts of  $\langle V, U \rangle$ . It is closely related to the Power of One Qubit (POOQ) [20], a circuit that computes the trace of a unitary  $U$  by implementing the controlled- $U$  gate with a single ancilla. In fact, it directly generalizes the POOQ, using two ancillas, and hence we call it the Power of Two Qubits (POTQ). Although the POTQ requires controlled versions of  $U$  and  $V$ , a key feature that keeps the depth short is that these controlled gates are performed in parallel. Interestingly, setting  $V$  to the identity in POTQ recovers the original POOQ.

When incorporated into QAQC, both of our circuits provide an exponential speedup over quantum compiling on a classical computer. Below we give detailed descriptions of our gradient-free and gradient-based methods for QAQC, which respectively employ our Hilbert-Schmidt Test and our POTQ circuits. Our QAQC method for training a gate sequence  $V$  involves optimizing over both the structure of the gate sequence (types of gates and their locations) as well as the continuous internal parameters inside the gates. Hence, this involves solving a hybrid discrete-continuous optimization problem.

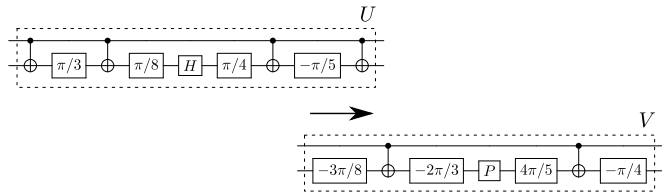
As a proof-of-principle, we implement our gradient-free QAQC on both IBM's and Rigetti's quantum computers, and we compile various one-qubit gates to the native gate alphabets used by these hardwares. In addition, we compile single and multi-qubit gates using a simulator with both our gradient-free and gradient-based methods. Although the noise level of current NISQ hardware prevents us from compiling multi-qubit gates with our QAQC method, we are optimistic that slight improvements in the noise will enable this application.

In what follows, we first discuss several applications of interest for QAQC. Section III presents our main results: our short-depth circuits for cost evaluation on a quantum computer. Section IV outlines our gradient-free and gradient-based methods for QAQC. Finally, Sections V and VI, respectively, discuss the implementations of our compiling methods on quantum hardware and a simulator.

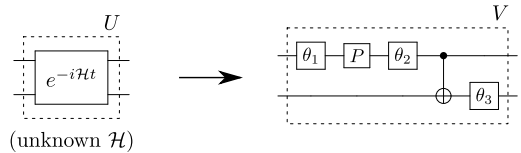
## II. APPLICATIONS OF QAQC

Figure 1 illustrates four potential applications for QAQC. Suppose that you know a quantum algorithm to perform some task, but the gate sequence is too long. As shown in Fig. 1(a), QAQC could be used to shorten the gate sequence (e.g., by accounting for the NISQ constraints of the particular hardware).

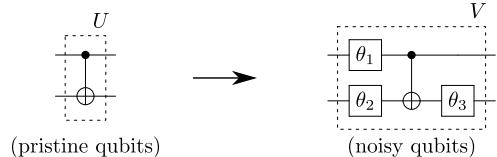
(a) SHORT-DEPTH COMPILING



(b) BLACK-BOX UPLOADING



(c) NOISE-TAILORED ALGORITHMS



(d) BENCHMARKING

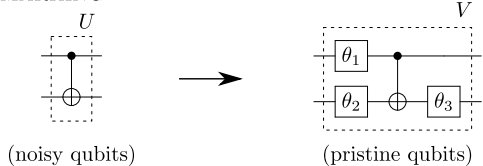


FIG. 1: Potential applications of QAQC. Here,  $\boxed{\theta}$  denotes rotation  $R_z(\theta)$ , while  $\boxed{P}$  represents  $\pi/2$ -pulse given by  $R_x(\pi/2)$ . Both gates are natively implemented on commercial hardware [21, 22]. (a) Compiling a given unitary  $U$  to a short-depth gate sequence  $V$  in terms of native hardware gates. (b) Uploading a black-box unitary. The black box could be an analog unitary,  $U = e^{-iHt}$  for an unknown Hamiltonian  $\mathcal{H}$ , that one wishes to convert into a gate sequence to be run on a gate-based quantum computer. (c) Compiling algorithms in the presence of noise to learn a new algorithm that counteracts the noise. Here, the unitary  $U$  is performed on high quality qubits and  $V$  is performed on noisy ones. (d) Benchmarking a quantum computer by compiling a unitary  $U$  on noisy qubits and learning the gate sequence  $V$  on high quality qubits.

Alternatively, suppose that you have a quantum computer and another quantum system, whose Hamiltonian  $\mathcal{H}$  you do not know. Nevertheless, you want to simulate the evolution of your quantum system (via  $e^{-iHt}$ ) but on your quantum computer. We call this situation black-box uploading, because you have a black box ( $e^{-iHt}$ ) that you want to upload onto your quantum computer. This is depicted in Fig. 1(b). QAQC could be used for black-box uploading by converting your black box into a gate sequence on your quantum computer.

Finally, we highlight two additional applications that are the opposites of each other. These two applications can be exploited when your quantum computer has some good qubits (qubits with low noise) and some bad qubits (qubits with high noise).

Consider Fig. 1(c). Here, your goal is to implement a CNOT on two noisy qubits. But to actually implement a true CNOT, you will need to physically implement a dressed CNOT, i.e., a CNOT dressed by one-qubit unitaries. QAQC can allow you to train the parameters in these one-qubit unitaries. By choosing your target unitary  $U$  to be a CNOT on a pristine (i.e., noiseless) pair of qubits, you can learn the unitary  $V$  on your noisy qubits that you would need to effectively implement a CNOT. We call this application noise-tailored algorithms, since you are learning an algorithm that is robust to the noise process on your noisy qubits.

Figure 1(d) depicts the opposite process, which is benchmarking. Here, you have a unitary  $U$  acting on a noisy set of qubits, and you want to know what the equivalent unitary  $V$  would be if it were implemented on a pristine set of qubits. This essentially corresponds to learning the noise model, i.e., benchmarking your noisy qubits.

### III. OUR CIRCUITS

Here we present our main results: short-depth circuits for evaluating the cost in Eq. (1). We note that these circuits are also interesting outside of the scope of QAQC, and they likely have applications in other areas.

#### A. Hilbert-Schmidt Test

Consider the circuit in Fig. 2. Below we show that this circuit computes  $|\text{Tr}(V^\dagger U)|$  where  $U$  and  $V$  are  $d$ -dimensional unitary matrices. Defining  $n := \log_2 d$ , the circuit involves  $2n$  qubits, where we call the first (second)  $n$  qubits system  $A$  (system  $B$ ).

The first step is to create a maximally entangled state between  $A$  and  $B$ , namely the state

$$|\Phi^+\rangle = \frac{1}{\sqrt{d}} \sum_j |j\rangle_A \otimes |j\rangle_B, \quad (2)$$

where  $\mathbf{j} = (j_1, j_2, \dots, j_n)$  is a vector index where each component  $j_k$  is chosen from  $\{0, 1\}$ . The first two gates in Fig. 2 - the Hadamard gates and the CNOT gates (which are performed in parallel when on distinct qubits) - create the  $|\Phi^+\rangle$  state.

The second step is to act with  $U$  on system  $A$  and  $V^*$  on system  $B$ . ( $V^*$  is the complex conjugate of  $V$ , where the complex conjugate is taken in the standard basis.) Note that these two gates are performed in parallel. This gives the state

$$(U \otimes V^*)|\Phi^+\rangle = \frac{1}{\sqrt{d}} \sum_j U|j\rangle_A \otimes V^*|j\rangle_B. \quad (3)$$

The third and final step is to measure in the Bell basis. This corresponds to undoing the unitaries (the CNOTs

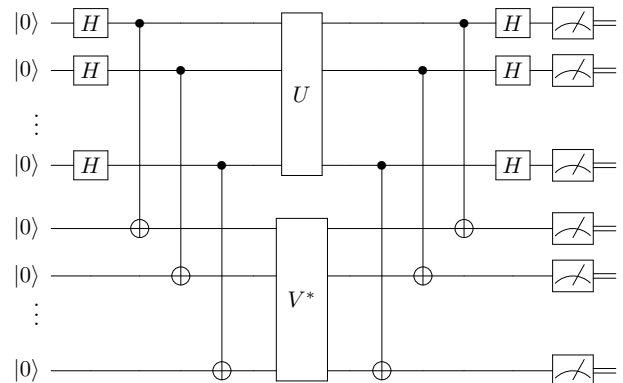


FIG. 2: Hilbert-Schmidt Test. For this circuit, the probability to obtain the measurement outcome where all qubits are in the  $|0\rangle$  state is equal to  $(1/d^2)|\text{Tr}(V^\dagger U)|^2$ . Hence this circuit computes the magnitude of the Hilbert-Schmidt inner product  $|\langle V, U \rangle|$  between two  $d$ -dimensional unitaries  $U$  and  $V$ .

and Hadamards) used to prepare  $|\Phi^+\rangle$  and then measuring in the standard basis. In the end, we are only interested in estimating a single probability: the probability for the Bell-basis measurement to give the  $|\Phi^+\rangle$  outcome (corresponding to the all-zeros outcome in the standard basis). The amplitude associated with this probability is

$$\langle \Phi^+ | U \otimes V^* | \Phi^+ \rangle = \langle \Phi^+ | UV^\dagger \otimes \mathbb{1} | \Phi^+ \rangle \quad (4)$$

$$= \frac{1}{d} \text{Tr}(V^\dagger U). \quad (5)$$

To obtain the first equality we used the ricochet property:

$$X \otimes \mathbb{1} | \Phi^+ \rangle = \mathbb{1} \otimes X^T | \Phi^+ \rangle, \quad (6)$$

which holds for any operator  $X$  acting on a  $d$ -dimensional space. The probability of the  $|\Phi^+\rangle$  outcome is then the absolute square of the amplitude, which gives a probability of  $(1/d^2)|\text{Tr}(V^\dagger U)|^2$ . Hence, this probability gives us the absolute value of the Hilbert-Schmidt inner product between  $U$  and  $V$ . We therefore call the circuit in Fig. 2 the Hilbert-Schmidt Test (HST).

Consider the depth of this circuit. Let  $D(G)$  denote the depth of a gate sequence  $G$  for a quantum computer whose native gate alphabet includes the CNOT gate and the set of all one-qubit gates. Then, for the HST, we have

$$D(\text{HST}) = 4 + \max\{D(U), D(V^*)\}. \quad (7)$$

The first term of 4 is associated with the Hadamards and CNOTs in Fig. 2, and this term is negligible when  $U$  or  $V$  is large. The second term denotes that  $U$  and  $V^*$  are performed in parallel, and hence whichever unitary has the larger depth will determine the overall depth of the HST.

## B. The Power of Two Qubits

While the HST only gives the magnitude of  $\langle V, U \rangle$ , we now consider a circuit that gives the real and imaginary parts. Before we discuss this circuit, let us review the Power of One Qubit (POOQ) [20], shown in Fig. 3(a), which is a circuit for computing the trace of a  $d$ -dimensional system  $A$  initially in the maximally mixed state,  $\mathbb{1}/d$ , and a single-qubit ancilla  $Q$  initially in the  $|0\rangle$  state. After applying a Hadamard to  $Q$  and a controlled- $U$  gate on  $QA$  (with  $Q$  the control system), the reduced density matrix  $\rho_Q$  has its off-diagonal element proportional to  $\text{Tr}(U)$ . Hence, one can measure  $Q$  in the  $X$  and  $Y$  bases, respectively, to read off the real and imaginary parts of  $\text{Tr}(U)$ .

Our circuit for computing  $\langle V, U \rangle$  generalizes the POOQ and is called the Power of Two Qubits (POTQ), depicted in Fig. 3(b). As the name suggests, the POTQ employs two qubit ancillas,  $Q$  and  $Q'$ , each initially in the  $|0\rangle$  state. In addition, two  $d$ -dimensional systems,  $A$  and  $B$ , are initially prepared in the Bell state  $|\Phi^+\rangle$  defined in Eq. (2). (Although not shown in Fig. 3(b), this Bell state is prepared with a depth-two circuit, as shown in Fig. 2.)

The first step in the POTQ is to prepare the two-qubit maximally entangled state  $\frac{1}{\sqrt{2}}(|0\rangle|0\rangle + |1\rangle|1\rangle)$  between  $Q$  and  $Q'$ , using a Hadamard and CNOT as shown in Fig. 3(b). The second step is to apply a controlled- $U$  gate between  $Q$  and  $A$  (with  $Q$  the control system). In parallel with this gate, the anticcontrolled- $V^T$  gate is applied to  $Q'B$ , with  $Q'$  the control system, where anticcontrolled means that the roles of the  $|0\rangle$  and  $|1\rangle$  states on the control system are reversed. This results in the state:

$$\begin{aligned} & \frac{1}{\sqrt{2}}(|0\rangle_Q|0\rangle_{Q'}(U \otimes \mathbb{1}_B)|\Phi^+\rangle \\ & + |1\rangle_Q|1\rangle_{Q'}(\mathbb{1}_A \otimes V^T)|\Phi^+\rangle) \\ & = \frac{1}{\sqrt{2}}(|0\rangle_Q|0\rangle_{Q'}(U \otimes \mathbb{1}_B)|\Phi^+\rangle \\ & + |1\rangle_Q|1\rangle_{Q'}(V \otimes \mathbb{1}_B)|\Phi^+\rangle). \end{aligned} \quad (8)$$

Here, the equality used the ricochet property in (6).

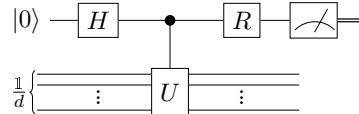
Finally, a CNOT gate is applied to  $QQ'$ , with  $Q$  the control system. This results in the reduced state on  $Q$  being

$$\begin{aligned} \rho_Q = \frac{1}{2} & (|0\rangle\langle 0| + \text{Tr}(V^\dagger U)|0\rangle\langle 1| \\ & + \text{Tr}(U^\dagger V)|1\rangle\langle 0| + |1\rangle\langle 1|). \end{aligned} \quad (9)$$

By inspection of  $\rho_Q$ , one can see that measuring  $Q$  in the  $X$  and  $Y$  bases respectively gives the real and imaginary parts of  $\text{Tr}(V^\dagger U)$ .

Interestingly, if we set  $V$  to the identity in the POTQ, then since the CNOT gate commutes with the controlled- $U$  gate and the reduced state of  $|\Phi^+\rangle$  is the maximally

### (a) POWER OF ONE QUBIT



### (b) POWER OF TWO QUBITS

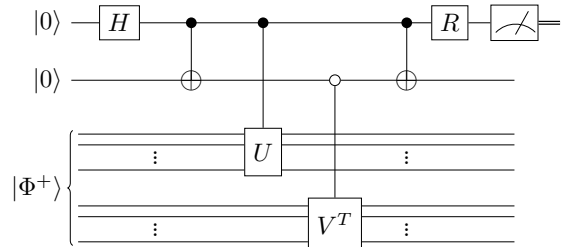


FIG. 3: **(a)** The Power of One Qubit (POOQ) [20]. This can be used to compute the trace of a unitary  $U$  acting on a  $d$ -dimensional space. The  $R$  gate represents either  $H$ , in which case the circuit computes  $\text{Re}[\text{Tr}(U)]$ , or the  $S$  gate followed by  $H$ , in which case the circuit computes  $\text{Im}[\text{Tr}(U)]$ . **(b)** The Power of Two Qubits (POTQ). This is a generalization of the POOQ, as can be seen by setting  $V = \mathbb{1}$ . The POTQ can be used to compute the Hilbert-Schmidt inner product  $\text{Tr}(V^\dagger U)$  between two unitaries  $U$  and  $V$  acting on a  $d$ -dimensional space. As with the POOQ,  $R = H$  leads to  $\text{Re}[\text{Tr}(UV^\dagger)]$ , while a  $R = HS$  leads to  $\text{Im}[\text{Tr}(UV^\dagger)]$ .

mixed state  $\frac{1}{d}$ , we recover the POOQ. The POTQ is therefore a generalization of the POOQ.

Note that while the POOQ can also be used to determine  $\text{Tr}(V^\dagger U)$ , the POTQ has the advantage that the controlled gates for  $U$  and  $V$  can be executed in parallel, while in the POOQ they would have to be executed in series. This makes the POTQ better suited for NISQ devices, where short depth is crucial. Consider the depth of the POTQ. Denoting the controlled- $U$  and the anticcontrolled- $V^T$  as  $C_U$  and  $\bar{C}_{V^T}$  respectively, the overall depth is

$$D(\text{POTQ}) = 4 + \max\{D(C_U), D(\bar{C}_{V^T})\} \quad (10)$$

Note the similarity here to Eq. (7). The overall depth is essentially determined by whichever controlled gate has the largest depth.

## IV. OUR OPTIMIZATION METHOD

In this section, we give a detailed description of our optimization method for QAQC. First we discuss how we parameterize the trainable unitary  $V$ , in terms of both discrete and continuous parameters. Then we present our two different approaches to optimizing over the continuous parameters: a gradient-free approach (which employs the circuit in Fig. 2) and a gradient-based approach (which employs the circuit in Fig. 3).

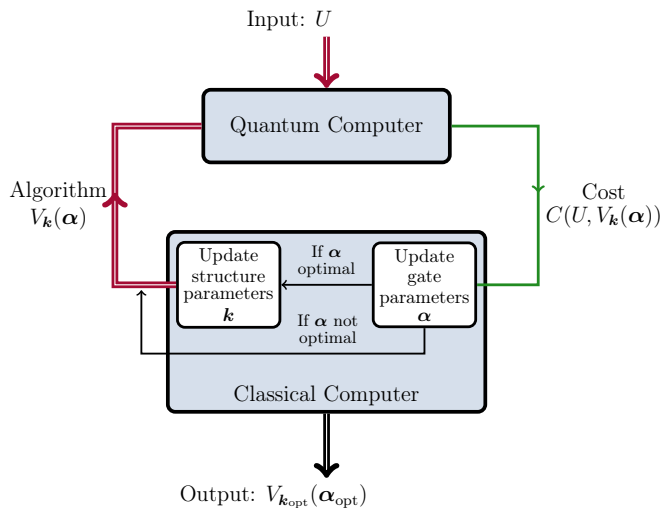


FIG. 4: Outline of our approach to optimization over gate structures and continuous gate parameters in order to compile the input unitary  $U$  to the native gate set  $\{G_k(\alpha)\}_k$  of a quantum computer. The optimization starts with a random choice of gate structure followed by a continuous optimization over the internal gate parameters. After obtaining the optimal gate parameters, the structure is updated and the internal gate parameters are optimized again, followed by another structure update. This process repeats until the cost reaches its minimum.

### A. Discrete and continuous parameters

Consider an alphabet  $\mathcal{A} = \{G_k(\alpha)\}_k$  of gates  $G_k(\alpha)$  that are native to the quantum computer of interest. Here,  $\alpha \in \mathbb{R}$  is a continuous parameter, and  $k$  is a discrete parameter that identifies the type of gate and which qubits it acts on. For a given quantum computer, the problem of compiling  $U$  to a gate sequence of length  $L$  is to determine

$$(\alpha_{\text{opt}}, \mathbf{k}_{\text{opt}}) := \arg \min_{(\alpha, \mathbf{k})} C(U, V_{\mathbf{k}}(\alpha)), \quad (11)$$

where

$$V_{\mathbf{k}}(\alpha) = G_{k_L}(\alpha_L) G_{k_{L-1}}(\alpha_{L-1}) \cdots G_{k_1}(\alpha_1), \quad (12)$$

is the trainable unitary, which is a function of the sequence  $\mathbf{k} = (k_1, \dots, k_L)$  of parameters describing which gates from the native gate set are used and of the continuous parameters  $\alpha = (\alpha_1, \dots, \alpha_L)$  corresponding to each gate. The function  $C(U, V_{\mathbf{k}}(\alpha))$  is the cost, which describes how close the trained unitary is to the target unitary and is minimized if and only if the trained unitary matches the target up to a global phase factor.

The optimization in (11) contains two parts: discrete optimization over the finite set of gate structures parameterized by  $\mathbf{k}$ , and continuous optimization over the parameters  $\alpha$  characterizing the gates within the structure. Our quantum-classical hybrid strategy to perform the optimization in (11) is illustrated in Fig. 4. As the set of

gate structures grows exponentially with the number of gates  $L$ , a brute force search over all gate structures in order to obtain the best one is intractable in general. To efficiently search through this exponentially large space, we adopt an approach based on simulated annealing: we start with a random gate structure, then perform continuous optimization over the parameters  $\alpha$  that characterize the gates such that the cost function is minimized. We then randomly substitute a subset of gates  $\{G_{k_i}(\alpha_{k_i})\}_{i=1}^m$  in the original sequence and re-optimize the cost function over the continuous parameters  $\alpha$ . If this change produces a lower cost, we accept the change. If the cost increases, we accept the change with probability decreasing exponentially in the magnitude of the cost difference. We iterate this procedure until the cost is (sufficiently close to) zero or until a maximum number of iterations is reached.

To perform the continuous optimization over the gate parameters, we use both a gradient-free approach and a gradient-based approach. Our gradient-free approach is based on a cost function defined by the Hilbert-Schmidt Test, while our gradient-based approach uses a cost function defined by the POTQ.

### B. Gradient-free compiling

In the gradient-free approach to optimizing over the continuous gate parameters  $\alpha$ , we take as our cost function

$$C_{\text{GF}}(U, V_{\mathbf{k}}(\alpha)) := 1 - \frac{1}{d} |\text{Tr}(V_{\mathbf{k}}(\alpha)^\dagger U)|, \quad (13)$$

and we compute this using the Hilbert-Schmidt test as illustrated in Fig. 2. Note that for any two unitaries  $U$  and  $V$ ,  $C_{\text{GF}}(U, V) = 0$  if and only if  $U$  and  $V$  differ by a global phase factor, i.e.,  $V = e^{i\varphi}U$  for some  $\varphi \in \mathbb{R}$ . By minimizing  $C_{\text{GF}}$ , we thus learn an equivalent unitary  $V$  up to global phase.

For a given set of gate structure parameters  $\mathbf{k}$ , the calculation of the cost on a quantum computer (as well as a simulator) is affected by the fact that, due to finite sampling, the Hilbert-Schmidt Test allows us to obtain only an estimate of the modulus of the Hilbert-Schmidt inner product. Noise within the quantum computer itself also affects the calculation of the cost. Therefore, in order to perform gradient-free optimization over the continuous internal gate parameters  $\alpha$ , we make use of stochastic optimization techniques that are designed to optimize random functions. Specifically, we make use of the `gp_minimize` routine in the `scikit-optimize` Python library [23], which is a gradient-free optimization routine that performs Bayesian optimization using Gaussian processes [24, 25]. See Algorithm 1 for a general overview of the optimization procedure.

In Appendix A, Algorithm 3, we propose an alternative algorithm for gradient-free quantum optimization that, on average, significantly reduces the number of calls to

---

**Algorithm 1:** GRADIENT-FREE  
CONTINUOUS OPTIMIZATION FOR QAQC

---

**Input:** Unitary  $U$  to be compiled; trainable unitary  $V_{\mathbf{k}}(\boldsymbol{\alpha})$  of a given structure; error tolerance  $\text{tol} \in (0, 1)$ ; maximum number of iterations  $N$ ; sample precision  $\epsilon > 0$ .

**Output:** Parameters  $\boldsymbol{\alpha}_{\text{opt}}$  that minimize the cost  $C_{\text{GF}}$  at best to within  $\text{tol}$  of zero, i.e. where  $C_{\text{GF}}(U, V_{\mathbf{k}}(\boldsymbol{\alpha}_{\text{opt}})) \leq \text{tol}$ .

**Init:**  $\boldsymbol{\alpha}_{\text{opt}} \leftarrow 0$ ;  $\text{cost} \leftarrow 1$

- 1 **repeat**
- 2     choose an initial parameter  $\boldsymbol{\alpha}^0$  at random;
- 3     run `gp_minimize` with  $\boldsymbol{\alpha}^0$  as input and  $\boldsymbol{\alpha}_{\text{min}}$  as output; whenever the cost is called upon some  $\boldsymbol{\alpha}$ , run the HST on  $V_{\mathbf{k}}(\boldsymbol{\alpha})^*$  and  $U$  approximately  $1/\epsilon^2$  times to estimate the cost  $C_{\text{GF}}(V_{\mathbf{k}}(\boldsymbol{\alpha}), U)$
- 4     **if**  $\text{cost} \geq C_{\text{GF}}(U, V_{\mathbf{k}}(\boldsymbol{\alpha}_{\text{min}}))$  **then**
- 5          $\text{cost} \leftarrow C_{\text{GF}}(U, V_{\mathbf{k}}(\boldsymbol{\alpha}_{\text{min}}))$ ;  $\boldsymbol{\alpha}_{\text{opt}} \leftarrow \boldsymbol{\alpha}_{\text{min}}$
- 6 **until**  $\text{cost} \leq \text{tol}$  at most  $N$  times.
- 7 **return**  $\boldsymbol{\alpha}_{\text{opt}}$ ,  $\text{cost}$

---

the quantum computer. As a result, it is more suitable for cloud computing under a queue submission system (e.g., IBM’s Quantum Experience). This algorithm performs a “multi-scale bisection” of the parameter space based on simulated annealing.

We emphasize that our approach to gradient-free compiling avoids the exponential overhead of evaluating the cost function, yet at the same time makes use of fast and efficient classical heuristics for optimization. In fact, using the Hilbert-Schmidt Test, both Algorithm 1 and Algorithm 3 require only  $\tilde{O}(1/\epsilon^2)$  queries to the target unitary in order to evaluate the cost, where  $\epsilon = 1/\sqrt{n_{\text{shots}}}$  is the sample precision, which is related to the number of samples  $n_{\text{shots}}$  taken from the device.

A subtle point of gradient-free compiling via the Hilbert-Schmidt Test is that we compile  $V^*$ , not  $V$ . In many cases, translating the gate sequence  $V_{\mathbf{k}}(\boldsymbol{\alpha})^*$  to  $V_{\mathbf{k}}(\boldsymbol{\alpha})$  is trivial. For instance, suppose we are compiling a one-qubit gate  $U = X$  to a gate sequence in the alphabet  $\mathcal{A} = \{R_x(\pi/2), R_z(\theta)\}$  and end up with the exact decomposition  $V_{\mathbf{k}}(\boldsymbol{\alpha})^* = R_x(-\pi/2)R_x(-\pi/2)$ . Then, we simply have  $V_{\mathbf{k}}(\boldsymbol{\alpha}) = R_x(\pi/2)R_x(\pi/2) = V^*$ , an equivalent exact decomposition that retains the same depth as the compiled  $V^*$ . In other cases, the depth may be increased. Consider the artificial example of compiling the unitary  $U = R_x(-\pi/2)$  from the same gate alphabet  $\mathcal{A}$ . At depth 1, we would obtain  $V_{\mathbf{k}}(\boldsymbol{\alpha})^* = R_x(-\pi/2)$ . Then, in terms of the gate alphabet, we must add at least two gates  $V_{\mathbf{k}}(\boldsymbol{\alpha}) = R_x(\pi/2)R_x(\pi/2)R_x(\pi/2)$  or  $V_{\mathbf{k}}(\boldsymbol{\alpha}) = R_z(\pi)R_x(\pi/2)R_z(\pi)$  to obtain an exact decomposition, thereby increasing the depth of  $V$  by 2 relative to the depth of  $V^*$  [38]. We note that in practice the latter construction is preferable since frame changes  $R_z(\theta)$  are virtual gates and can be implemented “for free” with zero depth and zero noise on IBM’s hardware.

A first thought to get around this minor issue would

be to compile to the conjugate gate alphabet  $\mathcal{A}^* := \{G^* : G \in \mathcal{A}\}$  so that  $V_{\mathbf{k}}(\boldsymbol{\alpha})^* \subseteq \mathcal{A}^*$  guarantees that  $V_{\mathbf{k}}(\boldsymbol{\alpha}) \subseteq \mathcal{A}$ . This can be done on simulators with no problem, but on real quantum computers the gates must be compiled down to the actual gate alphabet before running on the device. Instead, we allow access to a small-scale classical compiler as a means of post-processing. This compilation procedure is efficient as it scales only linearly in the depth of the circuit. Additionally, only single qubit gates need to be modified to other single qubit gates, so this post-processing can be thought of as a simple translation instead of a formal compilation procedure.

### C. Gradient-based compiling

In this section, we introduce a gradient method for continuous optimization based on the POTQ algorithm for computing  $\text{Tr}(V^\dagger U)$ . While recent work on gradient descent continuous-variable optimization has shown vast quantum speed-ups over classical variants [26–28], the majority of proposals still appear to be out of reach for implementations on NISQ devices, mainly due to their technical nature (quantum state representation, quantum Fourier transform, Grover searching, etc.). Instead, we focus on continuous quantum optimization procedures that are feasible on current quantum computers and leave further asymptotic improvements of our algorithms as an open problem.

For the cost function, we adopt the normalized Hilbert-Schmidt distance, and define

$$\begin{aligned} C_{\text{GB}}(U, V_{\mathbf{k}}(\boldsymbol{\alpha})) &:= \frac{1}{2d} \|U - V_{\mathbf{k}}(\boldsymbol{\alpha})\|_{\text{HS}}^2 \\ &= 1 - \frac{1}{d} \text{Re}[\text{Tr}(V_{\mathbf{k}}(\boldsymbol{\alpha})^\dagger U)]. \end{aligned} \quad (14)$$

Note that for any two unitaries  $U$  and  $V$ , the cost  $C_{\text{GB}}(U, V)$  is zero if and only if  $U = V$ . Contrary to the gradient-free cost function  $C_{\text{GF}}$ , this cost function does not vanish if  $U$  and  $V$  differ only by a global phase. Indeed, if  $V = e^{i\varphi}U$ , then  $C_{\text{GB}}(U, V) = 1 - \cos(\varphi)$ .

In order to avoid exponential overhead, it is crucial for our gradient-based method to evaluate the gradient of the cost function using a quantum algorithm. Notice that the POTQ allows us to compute  $\text{Re}[\text{Tr}(V_{\mathbf{k}}(\boldsymbol{\alpha})^\dagger U)]$  on a quantum computer. Similarly, since

$$\nabla_{\boldsymbol{\alpha}} C_{\text{GB}}(U, V_{\mathbf{k}}(\boldsymbol{\alpha})) = -\frac{1}{d} \text{Re}[\text{Tr}(\nabla_{\boldsymbol{\alpha}} V_{\mathbf{k}}(\boldsymbol{\alpha})^\dagger U)], \quad (15)$$

the POTQ can also be used to evaluate the gradient of the cost function on a quantum computer. Because  $V_{\mathbf{k}}(\boldsymbol{\alpha})$  acts as a linear operator on a  $d$ -dimensional space, the gradient over  $\boldsymbol{\alpha}$  is a well defined operation that is easily performed in terms of additional gates in its circuit description. This follows from the fact that the decomposition of any unitary gate (or circuit) ultimately contains

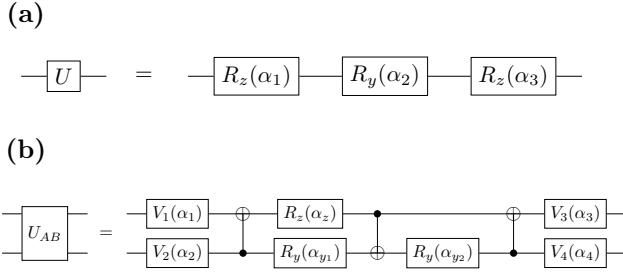


FIG. 5: (a) Any single-qubit gate  $U \in SU(2)$  can be decomposed into three elementary rotations (up to a global phase). Given appropriate parameters  $\alpha = (\alpha_1, \alpha_2, \alpha_3)$ ,  $U$  can be written as  $V(\alpha) = e^{-i\alpha_3\sigma_z/2}e^{-i\alpha_2\sigma_y/2}e^{-i\alpha_1\sigma_z/2}$ . (b) Any two-qubit gate  $U_{AB} \in SU(4)$  can be decomposed into 15 elementary single-qubit gates, as well as three CNOT gates. This decomposition is known to be optimal [29]. General universal quantum circuits for  $n$ -qubit gates are discussed in [30].

elementary single-qubit rotation gates of single continuous parameters. In that case, the derivatives can be computed by adding appropriate local Pauli gates prior to using the POTQ. Once the gradient is evaluated, it can then be supplied to a classical optimization procedure such as gradient descent.

---

**Algorithm 2:** GRADIENT-BASED  
CONTINUOUS OPTIMIZATION FOR QAQC

---

**Input:** Unitary  $U$  to be compiled; a trainable circuit  $V_{\mathbf{k}}(\alpha)$  of a given structure, where  $\alpha$  is a continuous circuit parameter of dimension  $L$ ; maximum number of iterations  $N$ ; error tolerance  $\text{tol} \in (0, 1)$ ; learning rate  $\eta > 0$ ; sample precision  $\epsilon > 0$ .

**Output:** Parameters  $\alpha_{\text{opt}}$  such that the optimized circuit  $V_{\mathbf{k}}(\alpha_{\text{opt}})$  minimizes the cost function  $C_{\text{GB}}(U, V_{\mathbf{k}}(\alpha_{\text{opt}})) = 1 - \frac{1}{d} \text{Re}[\text{Tr}(V_{\mathbf{k}}(\alpha_{\text{opt}})^\dagger U)]$  to within at best  $\text{tol}$  of zero.

**Init:**  $\alpha_{\text{opt}} \leftarrow 0$ ;  $\text{cost} \leftarrow 1$

```

1 repeat
2   choose initial parameters  $\alpha^0$  at random
3   for  $\tau = 1, 2, \dots, T$  do
4     for  $i = 1, 2, \dots, L$  do
5       run the POTQ on  $\nabla_i V_{\mathbf{k}}(\alpha^{\tau-1})^*$  and  $U$ 
           approximately  $1/\epsilon^2$  times to estimate
            $\text{Re}(\text{Tr}[\nabla_i V_{\mathbf{k}}(\alpha^{\tau-1})^\dagger U])$ 
6       update  $\alpha^\tau \leftarrow \alpha^{\tau-1} - \eta \nabla C(U, V_{\mathbf{k}}(\alpha^{\tau-1}))$ 
7   run the POTQ on  $V_{\mathbf{k}}(\alpha^\tau)^*$  and  $U$  approximately
            $1/\epsilon^2$  times to estimate the cost  $C_{\text{GB}}(U, V_{\mathbf{k}}(\alpha^\tau))$ 
8   if  $\text{cost} \geq C_{\text{GB}}(U, V_{\mathbf{k}}(\alpha^\tau))$  then
9      $\text{cost} \leftarrow C_{\text{GB}}(U, V_{\mathbf{k}}(\alpha^\tau))$ ;  $\alpha_{\text{opt}} \leftarrow \alpha^\tau$ 
10 until  $\text{cost} \leq \text{tol}$  at most  $N$  times
11 return  $\alpha_{\text{opt}}, \text{cost}$ 

```

---

Given an arbitrary black-box (controlled) unitary as input, Algorithm 2 compiles a circuit  $V_{\mathbf{k}}(\alpha)$  of given structure to a set of (locally) optimal parameters  $\alpha_{\text{opt}}$  that minimize the cost, i.e. the Hilbert-Schmidt dis-

tance, with respect to the target unitary. The gradient is evaluated with the POTQ circuit as a subroutine within a classical gradient descent algorithm. The overall query complexity of Algorithm 2 is  $\tilde{O}(NTL/\epsilon^2)$ , where  $\epsilon = 1/\sqrt{n_{\text{shots}}}$  is the sample precision,  $N$  is the maximum number of repetitions over random initial parameters  $\alpha^0$ ,  $L$  is the dimension of the continuous parameter space of  $\alpha$  and  $T$  is the number of gradient ascent iterations for a suitable learning rate  $\eta > 0$ . In order to improve convergence, it may also be useful to supply the quantum subroutines for computing the cost function and the gradient to a more advanced stochastic optimizer, for example as found in the Python library SciPy [31]. We give results on compiling both single-qubit and two-qubit gates on a simulator in Section VI.

When performing gradient-based optimization over an arbitrary target unitary in Algorithm 2, we rely on the ability to perform controlled operations of arbitrary (possibly unknown) gates. In general, in order to perform a controlled black-box operation with respect to the desired target unitary, one can use a method that doubles the size of the  $d$ -dimensional Hilbert space [32]. The method introduces a set of ancillas for each controlled qubit. One then uses two controlled-SWAP operations (per qubit/ancilla pair) prior and after querying the target unitary in order to realize a controlled black-box operation.

For the circuits studied below, we do not use this form of ‘remote control’. In practice, since any controlled unitary gate can be decomposed into native gates, the ability to compile the set of controlled rotations and SWAP, as well as the Toffoli gate, is sufficient. In order to account for this feature, we also assume a small-scale classical compiler to perform such a translation. While this may cause the depth of our circuit optimization to increase slightly, it does not pose any additional technical challenges for compiling. In fact, the required translation can be done manually and only requires introducing an additional gate set of constant depth.

We emphasize that our approach also succeeds without explicitly searching over structures. Due to the existence of exact universal circuits for  $n$ -qubit unitary operations [30], our gradient-based QAQC approach can, in principle, directly learn an arbitrary unitary gate at the cost of suboptimal depth. We give examples of universal circuits in Fig. 5.

## V. IMPLEMENTATION ON QUANTUM HARDWARE

In this section, we present the results of executing our QAQC procedure described in Sec. IV on IBM’s and Rigetti’s quantum computers. In each case, we performed gradient-free continuous parameter optimization in order to minimize the cost function  $C_{\text{GF}}$  in (13), evaluating this cost function at each iteration on the quantum computer.

### A. IBM's quantum computer

The native gate set of IBM's five-qubit quantum computer IBMQX4 is [33]

$$\mathcal{A}_{\text{IBMQX4}} = \{R_x(\pi/2), R_z(\theta), \text{CNOT}_{0,1}, \text{CNOT}_{0,2}, \text{CNOT}_{1,2}, \text{CNOT}_{2,3}, \text{CNOT}_{2,4}, \text{CNOT}_{3,4}\}. \quad (16)$$

To compile arbitrary unitaries  $U$ , we use the general procedure outlined in Sec. IV. Specifically, we start with a random gate structure by selecting a gate sequence  $V$  from the gate alphabet in (16). We then calculate the cost  $C_{\text{GF}}(U, V)$  by executing the Hilbert-Schmidt Test shown in Fig. 2 on the quantum computer. To perform the continuous parameter optimization over the angles  $\theta$  of the  $R_z$  gates, instead of employing the optimization procedure outlined in Sec. IV B, we make use of Algorithm 3 outlined in the Appendix. This method is designed to limit the number of objective function calls to the quantum computer, which is an important consideration when using IBMQX4 since the queue submission system can require a significant time to evaluate many calls to the quantum computer.

After performing the continuous optimization, we update a fixed number of gates in the sequence  $V$ , and evaluate the cost of the new sequence. This defines one iteration. If the new overlap is greater than the previous overlap, we accept the change; if the new overlap is smaller, we accept the change with a probability decreasing exponentially in the magnitude of the difference in overlap.

In Fig. 6(a), we show results for compiling single qubit gates on IBMQX4. All gates ( $\mathbb{1}$ ,  $T$ ,  $X$ , and  $H$ ) converge asymptotically to a cost below 0.1, but no gates achieve zero cost. This is due to a combination of finite sampling, gate and qubit fidelity, and readout errors on the device and not our method. Indeed, all gates compile to textbook decompositions—e.g.,  $X = R_x(\pi/2)R_x(\pi/2)$ —and on a simulator the cost vanishes completely.

### B. Rigetti's quantum computer

The native gate set of Rigetti's eight-qubit quantum computer 8Q-Agave is [34]

$$\mathcal{A}_{\text{8Q-Agave}} = \{R_x(\pm\pi/2), R_z(\theta), \text{CZ}_{0,1}, \text{CZ}_{1,2}, \text{CZ}_{2,3}, \text{CZ}_{3,4}, \text{CZ}_{4,5}, \text{CZ}_{5,6}, \text{CZ}_{6,7}, \text{CZ}_{7,0}\}, \quad (17)$$

where the single-qubit gates  $R_x(\pm\pi/2)$  and  $R_z(\theta)$  can be performed on any qubit and, due to the connectivity of the qubits on the quantum computer, the two-qubit controlled-Z (CZ) gate can be performed between neighboring qubits.

To compile any given unitary  $U$  to a sequence of gates from this alphabet, we make use of the general procedure outlined in Sec. IV. Specifically, we perform random updates to the gate structure followed by continuous optimization over the parameters  $\theta$  of the  $R_z$  gates

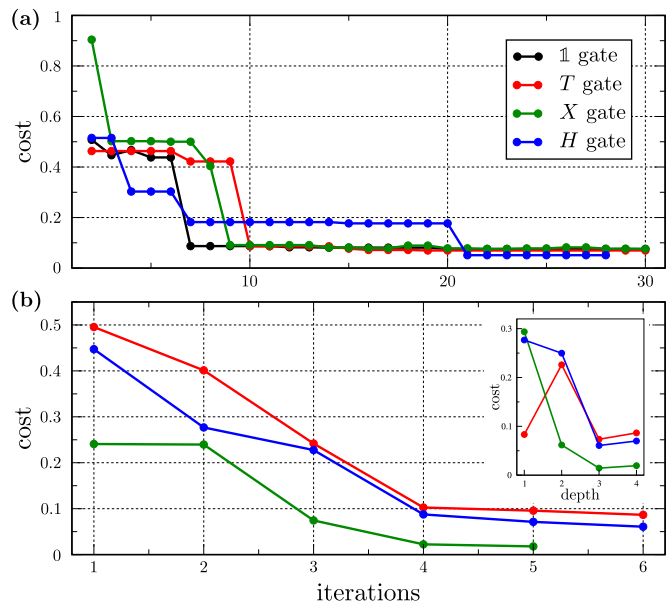


FIG. 6: Compiling one-qubit gates using the gradient-free optimization technique described in Sec. IV B. The plots show the cost as a function of the number of iterations of the full gate structure and continuous parameter optimization; see Sec. IV A for a description of the procedure. The cost tolerance parameter `tol` defined in Sec. IV B was set to  $10^{-2}$ . (a) Compiling the one-qubit gates  $\mathbb{1}$ ,  $X$ ,  $H$ , and  $T$  on the IBMQX4 quantum computer, in which we took  $n_{\text{shots}} = 8000$  to evaluate the cost at each iteration. (b) Compiling the one-qubit gates  $X$ ,  $H$ , and  $T$  on Rigetti's 8Q-Agave quantum computer. For each run of the Hilbert-Schmidt test to determine the cost, we took  $n_{\text{shots}} = 10,000$ . (Inset) The minimum cost achieved by optimizing over gate sequences with a fixed depth.

using the gradient-free stochastic optimization technique described in Sec. IV B, Algorithm 1. We took the cost error tolerance (the parameter `tol` in Algorithm 1) to be  $10^{-2}$ , and for each run of the Hilbert-Schmidt test, we let  $n_{\text{shots}} = 10,000$  in order to estimate the cost. Our results are shown in Fig. 6(b).

The gates compiled in Fig. 6(b) had the following optimal decompositions. The same decompositions also achieved the lowest cost in the cost vs. depth plot in the inset.

1.  $T$  gate:  $R_z(\theta)$ , with  $\theta \approx 0.249\pi$ .
2.  $X$  gate:  $R_x(-\pi/2)R_z(\theta)R_x(-\pi/2)$ , with  $\theta \approx 0$ .
3.  $H$  gate:  $R_z(\theta_1)R_x(-\pi/2)R_z(\theta_2)$ , with  $\theta_1 \approx 0.50\pi$  and  $\theta_2 \approx 0.49\pi$ .

As with the results on IBM's quantum computer, none of the gates achieve a cost less than  $10^{-2}$ , due to factors such as finite sampling, low gate and qubit fidelities, and readout errors.

### C. Limitations due to NISQ devices

On both IBM’s and Rigetti’s hardware, we are able to successfully compile one-qubit gates with no *a priori* assumptions about gate structure or parameters. To our knowledge, this is the first demonstration of QAQC with real quantum hardware. In principle, our approach extends to compiling larger unitaries  $U$  with an exponential speedup over classical methods. In practice, limitations arise in this approach due to decoherence, gate imperfections, and readout errors on near-term quantum computers.

These limitations are more pronounced as circuit depth increases. We therefore encounter significant performance loss for controlled unitaries as required in the POTQ circuit. Consequently, we did not implement our gradient-based optimization method on current quantum devices, but we speculate that improvements to quantum computers will enable this application.

A qualitative noise analysis of the Hilbert-Schmidt Test circuit (Fig. 2) is as follows. To compile a unitary  $U$  acting on  $n$  qubits, a circuit with  $2n$  qubits is needed. Preparing the maximally-entangled state  $|\Phi^+\rangle$  in the first portion of the circuit requires  $n$  CNOT gates, which are significantly noisier than one qubit gates and propagate errors to other qubits through entanglement. In principle, all Hadamard and CNOT gates can be implemented in parallel, but on near-term devices this may not be the case. Additionally, due to limited connectivity of NISQ devices, it is generally not possible to directly implement CNOT between arbitrary qubits. Instead, the CNOT’s need to be “chained” between qubits that are connected, a procedure that can significantly increase the depth of the circuit.

The next level of the circuit involves implementing  $U$  in the top register and  $V^*$  in the bottom register, each of which act on  $n$  qubits. Here, the noise of the computer on  $V^*$  is not necessarily undesirable since it could allow us to compile noise-tailored algorithms that counteract the noise of the specific computer. Nevertheless, the depth of  $V^*$  and/or  $U$  essentially determines the overall circuit depth as noted in (7), and quantum coherence decays exponentially with the circuit depth. Hence, compiling larger gate sequences involves additional loss of coherence on NISQ computers.

The final level of the circuit involves making a Bell measurement on all qubits and is the reverse of the first part of the circuit. As such, the same noise analysis of the first portion of the circuit applies here. Readout errors can be significant on NISQ devices [35], and our circuit involves a number of measurements that scales linearly in the number of qubits. Hence, compiling larger unitaries increases overall readout error.

For all of these reasons, we limit implementation on real quantum devices to one-qubit gates. This establishes a proof-of-principle of our methodology, and our approach will only improve as the engineering of quantum hardware improves. To demonstrate applications

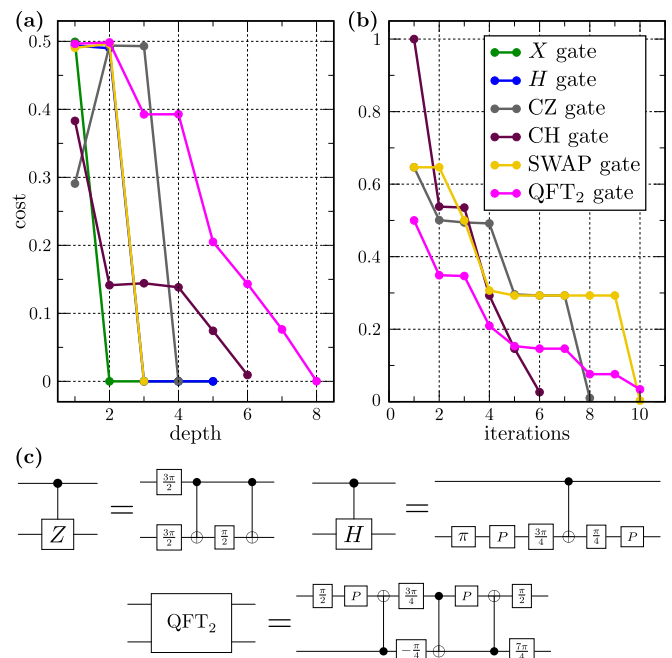


FIG. 7: Compiling one- and two-qubit gates on a simulator with IBM’s gate alphabet in (16) using the gradient-free optimization technique described in Sec. IV B. (a) The minimum cost achieved by optimizing over gate sequences with a fixed depth. (b) The cost as a function of the number of iterations of the full gate structure and continuous parameter optimization; see Sec. IV A for a description of the procedure. (c) Shortest-depth decompositions of the two-qubit controlled- $Z$ , controlled-Hadamard, and quantum Fourier transform gates as determined by the compilation procedure. The optimizations were performed on Rigetti’s quantum virtual machine. Here,  $-\theta$  denotes the rotation gate  $R_z(\theta)$ , while  $-P$  represents the rotation gate  $R_x(\pi/2)$ .

on future devices, we now show examples for compiling larger unitaries by running the Hilbert-Schmidt Test and POTQ circuits on simulators.

## VI. IMPLEMENTATION ON SIMULATOR

In this section, we present our results on finding shortest-depth algorithms for single-qubit and two-qubit gates using a simulator. We used the gate alphabet defined in Eq. (16) (allowing for full and perfect connectivity between the qubits) and adopted the methods from Sec. IV B and IV C to perform the continuous-parameter optimization. It is worth emphasizing that we performed the simulation assuming no gate errors and no decoherence. Although we do not obtain the exponential advantages of running our algorithms on a quantum computer, these assumptions allow us to learn and compile larger unitaries.

*a. Gradient-free optimization.* Using Rigetti’s quantum virtual machine [21], we compiled the controlled-Hadamard (CH) gate, CZ gate, and the

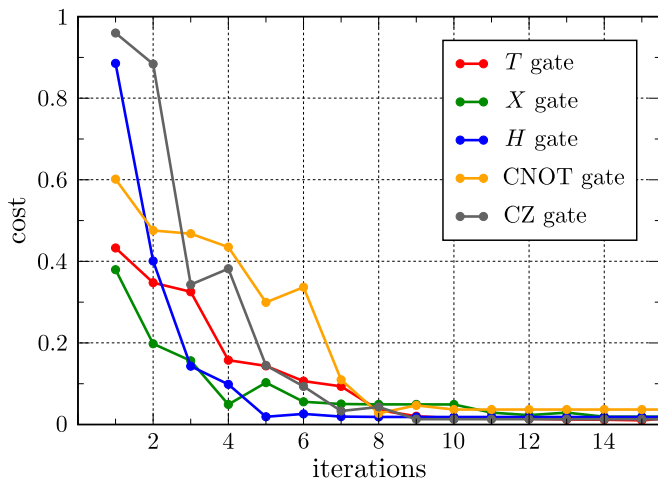


FIG. 8: Gradient-based quantum compilation for single-qubit and two-qubit gates into IBM’s native gate alphabet using a simulator. Algorithm 2 is run on a sample precision of  $n_{\text{shots}} = 10,000$ . Here, the cost refers to the normalized Hilbert-Schmidt distance with respect to the target gate.

two-qubit Fourier transform  $\text{QFT}_2$  by adopting the continuous optimization procedure in Algorithm 1. Using IBM’s simulator [22], we ran the bisection method in Algorithm 3 to compile the SWAP gate. For each run of the Hilbert-Schmidt test to determine the cost, we took  $n_{\text{shots}} = 20,000$ . Our results are shown in Fig. 7. For the SWAP gate, we find that circuits of depth one and two cannot achieve zero cost, but there exists a circuit with depth three for which the cost vanishes. The circuit achieving this zero cost is the well-known decomposition of the SWAP gate into three CNOT gates. While our compilation procedure reproduces the known decomposition of the SWAP gate, it discovers a decomposition of both the CZ and the  $\text{QFT}_2$  gates that differs from their conventional “textbook” decompositions, as shown in Fig. 7(c). In particular, these decompositions have shorter depths than the conventional decompositions when written in terms of the gate alphabet  $\{R_x(\pi/2), R_z(\theta), \text{CNOT}_{i,j}\}$  used here.

*b. Gradient-based optimization.* We used IBM’s simulator to compile a selection of single-qubit and two-qubit gates by performing the continuous optimization procedure in Algorithm 2. We compiled the  $T$  gate, the  $X$  gate and Hadamard ( $H$ ) gate, as well as CNOT and CZ gates, with a finite sample precision of  $n_{\text{shots}} = 10,000$ , as shown in Fig. 8. Increasing the number of shots to higher orders of magnitude significantly reduces the sampling error and results in more stable convergence at the cost of an increase in runtime.

## VII. CONCLUSIONS

Quantum compiling is crucial in the NISQ era, where NISQ constraints (limited connectivity, limited circuit depth, etc.) place severe restrictions on the quantum algorithms that can be implemented in practice. In this work, we presented a methodology for quantum assisted quantum compiling (QAQC), whereby a quantum computer provides an exponential speedup in evaluating the cost of a gate sequence, i.e., how well the gate sequence matches the target. In principle, QAQC should allow for compiling of larger algorithms than standard classical methods for quantum compiling, due to this exponential speedup. As a proof-of-principle, we implemented QAQC on IBM’s and Rigetti’s quantum computers to compile various one-qubit gates to their native gate alphabets. Current noise levels in the hardware prevented us from compiling multi-qubit gates, although we are optimistic that future noise reduction could enable larger scale QAQC.

Our main technical results were two short-depth circuits for computing the Hilbert-Schmidt inner product between a target unitary  $U$  and a trainable unitary  $V$ . One of these circuits computes the inner product magnitude, and we incorporated this circuit into our gradient-free QAQC method. The other circuit computes the real and imaginary parts of the inner product, and we exploited this circuit for gradient-based QAQC. The latter circuit generalized the famous Power of One Qubit [20] and hence is likely of interest to a broader community.

## VIII. ACKNOWLEDGEMENTS

We thank IBM and Rigetti for providing access to their quantum computers. The views expressed in this paper are those of the authors and do not reflect those of IBM and Rigetti. SK, RL, and AP acknowledge support from the U.S. Department of Energy through a quantum computing program sponsored by the LANL Information Science & Technology Institute. RL acknowledges support from an Engineering Distinguished Fellowship through Michigan State University. LC was supported by the U.S. Department of Energy through the J. Robert Oppenheimer fellowship. ATS and PJC were supported by the LANL ASC Beyond Moore’s Law project.

*Note added.* After completion of this work, we became aware of a recent paper [36] that presents various methods to train parameterized quantum circuits using quantum computers. While the goal is similar in spirit to our work, the approach is different from ours.

[1] Peter Shor. Polynomial-time algorithms for prime factorization and discrete logarithms on a quantum computer.

*SIAM Journal on Computing*, 26(5):1484–1509, 1997.  
[2] Edward Farhi, Jeffrey Goldstone, and Sam Gut-

- mann. A quantum approximate optimization algorithm. *arXiv:1411.4028*, 2012.
- [3] Richard P Feynman. Simulating physics with computers. *International journal of theoretical physics*, 21(6-7):467–488, 1982.
- [4] John Preskill. Quantum computing in the NISQ era and beyond. *arXiv:1801.00862*, 2018.
- [5] John Preskill. Quantum computing and the entanglement frontier. *arXiv:1203.5813*, 2012.
- [6] C Neill, P Roushan, K Kechedzhi, S Boixo, SV Isakov, V Smelyanskiy, R Barends, B Burkett, Y Chen, Z Chen, et al. A blueprint for demonstrating quantum supremacy with superconducting qubits. *arXiv:1709.06678*, 2017.
- [7] Davide Venturelli, Minh Do, Eleanor Rieffel, and Jeremy Frank. Compiling quantum circuits to realistic hardware architectures using temporal planners. *Quantum Science and Technology*, 3(2):025004, 2018.
- [8] Lukasz Cincio, Yiğit Subaşı, Andrew T Sornborger, and Patrick J Coles. Learning the quantum algorithm for state overlap. *arXiv:1803.04114*, 2018.
- [9] Dmitri Maslov, Gerhard W Dueck, D Michael Miller, and Camille Negrevergne. Quantum circuit simplification and level compaction. *IEEE Transactions on Computer-Aided Design of Integrated Circuits and Systems*, 27(3):436–444, 2008.
- [10] Yunseong Nam, Neil J Ross, Yuan Su, Andrew M Childs, and Dmitri Maslov. Automated optimization of large quantum circuits with continuous parameters. *arXiv:1710.07345*, 2017.
- [11] Jeffrey Booth Jr. Quantum compiler optimizations. *arXiv:1206.3348*, 2012.
- [12] Frederic T Chong, Diana Franklin, and Margaret Martonosi. Programming languages and compiler design for realistic quantum hardware. *Nature*, 549(7671):180, 2017.
- [13] Luke Heyfron and Earl T Campbell. An efficient quantum compiler that reduces  $t$  count. *arXiv:1712.01557*, 2017.
- [14] Thomas Häner, Damian S Steiger, Krysta Svore, and Matthias Troyer. A software methodology for compiling quantum programs. *Quantum Science and Technology*, 2018.
- [15] Angelo Oddi and Riccardo Rasconi. Greedy randomized search for scalable compilation of quantum circuits. In *International Conference on the Integration of Constraint Programming, Artificial Intelligence, and Operations Research*, pages 446–461. Springer, 2018.
- [16] Marcello Benedetti, Delfina Garcia-Pintos, Yunseong Nam, and Alejandro Perdomo-Ortiz. A generative modeling approach for benchmarking and training shallow quantum circuits. *arXiv:1801.07686*, 2018.
- [17] Peter D Johnson, Jonathan Romero, Jonathan Olson, Yudong Cao, and Alán Aspuru-Guzik. Qvector: an algorithm for device-tailored quantum error correction. *arXiv:1711.02249*, 2017.
- [18] Jarrod R McClean, Sergio Boixo, Vadim N Smelyanskiy, Ryan Babbush, and Hartmut Neven. Barren plateaus in quantum neural network training landscapes. *arXiv:1803.11173*, 2018.
- [19] Kosuke Mitarai, Makoto Negoro, and Keisuke Kitagawa, Masahiro nd Fujii. Quantum circuit learning. *arXiv:1803.00745*, 2018.
- [20] E. Knill and R. Laflamme. Power of one bit of quantum information. *Physical Review Letters*, 81:5672–5675, 1998.
- [21] Robert S Smith, Michael J Curtis, and William J Zeng. A practical quantum instruction set architecture. *arXiv:1608.03355*, 2016.
- [22] A. W. Cross, L. S. Bishop, J. A. Smolin, and J. M. Gambetta. Open Quantum Assembly Language. *arXiv:1707.03429*, 2017.
- [23] Scikit-optimize. <https://github.com/scikit-optimize/scikit-optimize>, 2018.
- [24] J. Močkus. On Bayesian methods for seeking the extremum. In *Optimization Techniques IFIP Technical Conference Novosibirsk, July 1–7, 1974*, pages 400–404, Berlin, Heidelberg, 1975. Springer Berlin Heidelberg.
- [25] Michael A. Osborne, Roman Garnett, and Stephen J. Roberts. Gaussian processes for global optimization. In *3rd International Conference on Learning and Intelligent Optimization (LION3) 2009*, 2009.
- [26] Patrick Reberstrost, Maria Schuld, Leonard Wossnig, Francesco Petruccione, and Seth Lloyd. Quantum gradient descent and newton’s method for constrained polynomial optimization. *arXiv:1612.01789*, 2016.
- [27] Iordanis Kerenidis and Anupam Prakash. Quantum gradient descent for linear systems and least squares. *arXiv:1704.04992*, 2017.
- [28] Andras Gilyen, Srinivasan Arunachalam, and Nathan Wiebe. Optimizing quantum optimization algorithms via faster quantum gradient computation. *arXiv:1711.00465*, 2017.
- [29] Farrokh Vatan and Colin Williams. Optimal quantum circuits for general two-qubit gates. *Phys. Rev. A*, 69:032315, Mar 2004.
- [30] P. B. M. Sousa and R. V. Ramos. Universal quantum circuit for  $n$ -qubit quantum gate: A programmable quantum gate. *Quantum Info. Comput.*, 7(3):228–242, March 2007.
- [31] Scipy optimization and root finding. <https://docs.scipy.org/doc/scipy/reference/optimize.html>, 2018.
- [32] Xiao-Qi Zhou, Timothy C. Ralph, Pruet Kalasuwan, Mian Zhang, Alberto Peruzzo, Benjamin P. Lanyon, and Jeremy L. O’Brien. Adding control to arbitrary unknown quantum operations. *Nature Communications*, 2(413), 2011.
- [33] IBM Q 5 Tenerife backend specification v1.1.0. <https://github.com/QISKit/qiskit-backend-information/tree/master/backends/tenerife/V1>, 2018.
- [34] Rigetti 8Q-Agave specification v.2.0.0.dev0. <http://docs.rigetti.com/en/latest/qpu.html>, 2018.
- [35] Abhinav Kandala, Kristan Temme, Antonio D. Corcoles, Antonio Mezzacapo, Jerry M. Chow, and Jay M. Gambetta. Extending the computational reach of a noisy superconducting quantum processor. *arXiv:1805.04492*, 2018.
- [36] Guillaume Verdon, Jason Pye, and Michael Broughton. A Universal Training Algorithm for Quantum Deep Learning. *arXiv:1806.09729*, 2018.
- [37] An exception to this is temporal planning [7] since it does not involve classical simulation of quantum dynamics but rather exploits commutation rules, which limits the gate alphabets that can be considered.
- [38] As in other places, when we speak about the depth from a gate alphabet, we only count gates from that gate alphabet.

### Appendix A: Alternative method for gradient-free optimization

An alternative approach to performing the continuous parameter optimization described in Sec. IV B is outlined in Algorithm 3. We implement this method, which is designed to limit the number of times the objective function is evaluated, specifically for the hardware of IBM because the queue submission system can require a significant time to make many calls to the quantum computer. In the discrete optimization procedure in Algorithm 3, we start with four angles spread uniformly in the interval  $[0, 2\pi)$ —namely  $0, \pi/2, \pi$ , and  $3\pi/2$ . This significantly reduces the size of the search space and allows us to get close to, or find exactly, an optimal gate sequence. Once the optimal structure is reached from this step, we then bisect the angles for each frame change  $R_z(\alpha)$  by evaluating the overlap with a new circuit containing  $R_z(\alpha \pm \pi/2^{t+1})$ , where  $t = 1, 2, \dots, t_{\max}$  is determined by the iteration in the procedure. Although we do not explore all angles in the interval, the runtime is logarithmically faster than a continuous search due to the bisection procedure. An additional advantage of this approach is that many gates have angles that are simple fractions of  $\pi$ , e.g.,  $T = R_z(\pi/4)$  and  $H = R_z(-\pi/2)R_x(-\pi/2)R_z(-\pi/2)$ . In a noiseless environment, the two steps above are sufficient. On actual devices, we implement a third step of stochastic optimization by evaluating the cost

for the new circuit with each frame change  $R_z(\alpha)$  replaced by  $R_z(\alpha \pm \Delta(t))$  for some small value  $\Delta(t) \ll 1$  decreasing monotonically with the iteration  $t$ . This allows us to compile for a given device by accounting for noise and gate errors. This can be thought of as a “fine-grained” angular optimization in contrast to the previous “coarse-grained” angular optimization.

---

#### Algorithm 3: GRADIENT-FREE OPTIMIZATION USING BISECTION FOR QAQC

---

**Input:** Unitary  $U$  to be compiled; trainable circuit  $V_{\mathbf{k}}$  of a given structure and gate alphabet  $\mathcal{A}$ ; error tolerance  $\text{tol} \in (0, 1)$ ; maximum number of iterations  $N$ ; maximum number of bisections  $t_{\max}$  of the unit circle; sample precision  $\epsilon > 0$ .

**Output:** Parameters  $\alpha_{\text{opt}}$  that minimize the cost  $C_{\text{GF}}$  at best to within  $\text{tol}$  of zero, i.e. where  $C_{\text{GF}}(V_{\mathbf{k}}(\alpha_{\text{opt}}), U) \leq \text{tol}$ .

**Init:** Restrict all gates in  $\mathcal{A}$  with continuous parameters to discrete angles in the set  $\Omega_0 = \{0, \pi/2, \pi, 3\pi/2\}$ ;  $\alpha_{\text{opt}} \leftarrow 0$ ;  $\text{cost} \leftarrow 1$

- 1 **for**  $t = 1, 2, \dots, t_{\max}$  **do**
- 2     **repeat**
- 3         anneal over all possible bisected angles in the set  $\Omega_t := \{\alpha \pm \pi/2^{t+1} \mid \text{for } \alpha \in \Omega_0\} \cup \Omega_{t-1}$ ;
- 4         whenever the cost is called upon some  $\alpha \in \Omega_t$ , run the HST on  $V_{\mathbf{k}}(\alpha)^*$  and  $U$  approximately  $1/\epsilon^2$  times to estimate the cost  $C_{\text{GF}}(V_{\mathbf{k}}(\alpha), U)$ ;
- 5         **if**  $\text{cost} \geq C_{\text{GF}}(V_{\mathbf{k}}(\alpha), U)$  **then**
- 6             |  $\text{cost} \leftarrow C_{\text{GF}}(V_{\mathbf{k}}(\alpha), U)$ ;
- 7         **until**  $\text{cost} \leq \text{tol}$  at most  $N$  times.
- 8     **repeat**
- 9         run `gp_minimize` to minimize the cost over all small continuous increments  $\Delta(t) \ll 1$  within the set of bisected angles  $\Omega_t$ ;
- whenever the cost is called on some  $\alpha + \Delta(t)$ , for  $\alpha \in \Omega_t$ , run the HST on  $V_{\mathbf{k}}(\alpha + \Delta(t))^*$  and  $U$  approximately  $1/\epsilon^2$  times to estimate the cost  $C_{\text{GF}}(V_{\mathbf{k}}(\alpha + \Delta(t)), U)$ ;
- 10         **if**  $\text{cost} \geq C_{\text{GF}}(V_{\mathbf{k}}(\alpha + \Delta(t)), U)$  **then**
- 11             |  $\text{cost} \leftarrow C_{\text{GF}}(V_{\mathbf{k}}(\alpha + \Delta(t)), U)$ ;
- |  $\alpha_{\text{opt}} \leftarrow \alpha + \Delta(t)$
- 12         **until**  $\text{cost} \leq \text{tol}$  at most  $N$  times.
- 13 **return**  $\alpha_{\text{opt}}, \text{cost}$

---